Bayesian constraints on pre-equilibrium jet quenching and predictions for oxygen collisions

Daniel Pablos [*]
IGFAE, Universidade de Santiago de Compostela, E-15782 Galicia-Spain Departamento de Física, Universidad de Oviedo, Avda. Federico García Lorca 18, 33007 Oviedo, Spain and Instituto Universitario de Ciencias y Tecnologías Espaciales de Asturias (ICTEA), Calle de la Independencia 13, 33004 Oviedo, Spain

Adam Takacs [†]
Institute for Theoretical Physics, Heidelberg University, Philosophenweg 16, 69120 Heidelberg, Germany

(Received 1 October 2025; accepted 13 March 2026; published 20 April 2026)

The contrast between the as-yet unmeasurable energy-loss effects in proton-nucleus collisions and the striking magnitude of the so-called high-momentum flow coefficients challenges our understanding of jet quenching mechanisms in large nucleus-nucleus collisions when applied to smaller systems. Intermediate-sized, light ion collisions will offer key insight into the system-size dependence of the interplay between jet energy loss and jet flow effects. To make quantitative predictions, we extend a semianalytic jet quenching framework by coupling it to state-of-the-art event-by-event hydrodynamics and, for the first time, incorporate pre-equilibrium energy loss via the hydrodynamic attractor. A Bayesian analysis shows that an early-time onset of energy loss is compatible with BNL Relativistic Heavy Ion Collider and CERN Large Hadron Collider measurements of jet suppression and jet elliptic flow in large systems, as well as hadron suppression, with the exception of hadron elliptic flow. Using these constraints, we predict both hadron and jet quenching observables in oxygen-oxygen collisions, finding sizable energy loss that exceeds the no-quenching baseline.

DOI: 10.1103/nw2z-pr7j

I. INTRODUCTION

Understanding the emergence of collective behavior in small collision systems, such as *pp* and *pA* collisions, remains one of the central challenges for both the high-energy physics and heavy-ion communities since their discovery at the CERN Large Hadron Collider (LHC) more than a decade ago [1–4] (for recent reviews, see [5–7]). While the dynamical origin of this collectivity is still under investigation, hydrodynamic models, originally thought to be valid only for large systems such as *AA* collisions, have proven quantitatively successful in describing several low-momentum observables in small systems as well [8–11] (a nonexhaustive list of alternative explanations includes [12–17]).

This hydrodynamic picture requires the presence of a deconfined quark-gluon plasma (QGP), implying final-state interactions and consequently jet quenching [18–20]. In *AA* collisions, jet modifications are firmly established, and their dependence on the medium size is consistent with expectations from parton energy-loss calculations performed using perturbative quantum chromodynamics (QCD) or holographic techniques [21–24]. However, in *pA* collisions, jet quenching remains elusive, possibly due to the short path lengths involved [25–28]. Despite the absence of measurable energy loss, significant azimuthal anisotropies have been observed in high-p_T particles in *pA* systems [29–31]. In *AA* collisions, this anisotropy is understood in terms of differences in energy loss due to the different path lengths traversed as a function of the jet orientation with respect to the reaction plane of the collision [32,33], adding further puzzling elements to the picture we attempt to draw for small systems.

Recent LHC runs on OO and NeNe collisions have provided a valuable bridge between small (*pp* and *pA*) and large (such as PbPb and AuAu) collision systems, thereby reducing uncertainties related to short path lengths and centrality determination [34–37]. In these smaller systems, fluctuations and out-of-equilibrium dynamics are believed to play an increasingly critical role in achieving quantitative precision [38–41].

In this work, we extend our semianalytic jet quenching framework [42–44] by incorporating these elements to enable reliable predictions for the upcoming experimental results on the potential existence of jet quenching effects in OO collisions. We account for medium fluctuations by coupling the framework to state-of-the-art event-by-event hydrodynamic simulations of the expanding fireball within which jets are produced and subsequently traverse. Before hydrodynamics is believed to be applicable, we incorporate quenching effects during the pre-equilibrium phase via the hydrodynamic attractor extracted from QCD kinetic theory, representing

[*]Contact author: pablosdaniel@uniovi.es
[†]Contact author: takacs@thphys.uni-heidelberg.de

Published by the American Physical Society under the terms of the Creative Commons Attribution 4.0 International license. Further distribution of this work must maintain attribution to the author(s) and the published article's title, journal citation, and DOI. Funded by SCOAP³.

the first time this is done in a realistic model for jet quenching.

We benchmark our model against a broad set of *AA* data, including both LHC and BNL Relativistic Heavy Ion Collider (RHIC) energies and collision systems, spanning wide ranges in centrality, jet cone size, and transverse momentum. Using Bayesian parameter estimation, we achieve a simultaneous and consistent description of jet suppression $R_{AA}^{\rm jet}(p_T)$ and elliptic anisotropy $v_2^{\rm jet}(p_T)$ across all available data. We show that the combination of $R_{AA}^{\rm jet}$ and $v_2^{\rm jet}$ provides constraints on energy-loss effects in the pre-equilibrium phase. The resulting posterior distributions can then be used to predict jet and hadron observables in other collision systems, including OO as we do in the present work.

II. FRAMEWORK

Our jet quenching framework builds on previous results from [42–44], which we briefly summarize here. We introduce two key new components: (i) the coupling to event-by-event fluctuating hydrodynamics, and (ii) energy loss in the pre-equilibrium phase using the hydrodynamic attractor.

Our starting point is the vacuum jet cross section, $\sigma_i^{pp}(p_T, R)$, computed using MadGraph + Pythia [45–47] at NLO + LL accuracy. We reconstructed jets and assigned their flavor ($i = q/g$) with the Flavor-kt [48]. Nuclear PDF (nPDF) effects are incorporated using EPPS21 [49] within the LHAPDF [50] framework, yielding the modified cross section $\tilde{\sigma}^{pp}(p_T, R)$. The charged hadron spectrum is evaluated by convoluting this jet spectrum with the NPC23 [51] fragmentation function (FF).

The quenched jet cross section is described via the convolution of the nPDF-modified jet cross section with the energy-loss probability distribution:

$$\sigma^{AA}(p_T, R) = \sum_{i=q,g} \int d\varepsilon P_i(\varepsilon, R, p_T) \tilde{\sigma}_i^{pp}(p_T + \varepsilon, R). \quad (1)$$

Energy is lost predominantly due to medium-induced emissions escaping the jet cone R, as encoded in $P_i(\varepsilon, R, p_T)$. The emission rate is computed using the improved opacity expansion in a static medium, which captures both single hard and multiple soft scatterings, and also includes finite path length corrections [52,53].[1] Medium properties affect these rates through LO hard thermal loop results, namely the (bare) jet quenching parameter $\hat{q}_0 = g_{\rm med}^2 N_c m_D^2 T/(4\pi)$, and the Debye screening mass $m_D^2 = 3g_{\rm med}^2 T^2/2$, where T is the local temperature of the hydrodynamic medium. Here, $g_{\rm med}$ is the (fixed, i.e., nonrunning) strong coupling for jet-medium interactions, representing the first of the two parameters we will estimate using Bayesian inference. We assume factorization between induced collinear emissions and transverse momentum broadening: semi-hard emissions undergo Gaussian broadening, while hard emissions inherit their transverse momentum from the Coulomb tail of the scattering potential. Since the softest emissions thermalize rapidly [56], they should be considered part of the medium and contribute to hydrodynamic wakes [57,58], a manifestation of medium response to the jet passage. We approximate these physics by assuming that the thermalized energy is distributed uniformly around the jet hemisphere. Elastic energy loss is also included and constrained via the Einstein relation $\hat{e} = \hat{q}/(4T)$, and is assumed to thermalize in a similar fashion. Here, $\hat{q}$ accounts for the logarithmic corrections of $\hat{q}_0$ (see later).

Energetic jets consist of multiple partons produced by the high-virtuality DGLAP evolution that occurs at the early stages of the in-medium jet propagation [59]. These partons represent an additional source of energy loss. We account for this by resumming these multiple sources via a factorization between early vacuum-like and medium-induced emissions [60]. Importantly, we also include color-coherence and color-resolution [61–63] effects (referred to as *coherent energy loss*) by incorporating the nonlocal angular scale below which the medium cannot resolve individual partons, $\theta_c \approx 1/\sqrt{\hat{q}L^3}$, with L being the traversed medium length. Detailed formulas are provided in [44].

Jet propagation occurs within an event-by-event fluctuating 2 + 1D hydrodynamic background. We employ hydroprofiles from the comprehensive multistage framework IP-Glasma + JIMWLK + MUSIC + UrQMD, which successfully describes a wide range of bulk observables in heavy-ion collisions [64]. This state-of-the-art framework evolves the bulk starting from the initial energy density deposited at specific hotspots determined by the IPSat [65]. Jet probes are placed precisely onto these hotspots, whose number is proportional to the number of binary collisions $N_{\rm coll}$, and their initial orientation is uniformly distributed in the azimuthal angle ϕ. Straight jet trajectories are sampled from their production point until they exit the deconfined medium at $T < T_c$, with T_c marks the crossover transition to the hadron gas phase. The medium and jet-medium interaction quantities needed for the computation of radiative and elastic energy loss are then obtained by averaging along each jet trajectory, as extracted from the hydrodynamic profiles. For example, we evaluate the Debye mass as $m_D^2 \propto (\int {\rm d}x_F T^2(x))/L$ for a given trajectory, where x_F is the distance traversed in the fluid rest frame, thereby accounting for different flow velocities, and L is the integral of ${\rm d}x_F$. The expressions for other relevant quantities can be found in Eq. (29) in [44]. We neglect further quenching below the freeze-out temperature T_c. For more details on the embedding of our jet quenching framework in the realistic heavy-ion environment, see Ref. [44], where event-averaged hydro profiles were used instead. Event classification into centrality classes is based on the final charged particle multiplicity of the bulk, from which one also extracts the soft event-plane angles Ψ_n, necessary for computing the jet flow coefficients. Thus, our framework predicts the quenched jet spectrum for various parameters $\sigma^{AA\%}(p_T, \eta, \phi, R)$.

The hydrodynamic description of the bulk begins at a finite time $\tau_{\rm hyd} = 0.4$ fm. This parameter was fixed when the IP-Glasma + JIMWLK + MUSIC + ultrarelativistic quantum molecular dynamics (UrQMD) framework was tuned to LHC and RHIC data. The initial condition of this nearly ideal fluid

[1] The static medium rates can mimic the rates of expanding medium in the multiple soft scattering limit [54,55].

is reached through the glasma evolution of saturated gluon fields. The glasma evolution should be followed by a kinetic evolution that drives the system toward hydrodynamics; however, this is not the setup used in the current bulk evolution framework. For reviews of this approach to thermalization, see [66,67]. Quenching effects have traditionally been neglected before $\tau_{\rm hyd}$, largely due to the absence of reliable energy-loss calculations in the nonequilibrated phases. While an earlier start could be mimicked by adjusting the jet-medium coupling, combined observables such as high-p_T R_{AA} and v_2 are known to be sensitive to the actual value of the quenching onset time [68,69]. The need to address jet quenching in the earliest stages has been emphasized in recent works where the pre-hydrophase is modeled either by Glasma [70,71] or by QCD effective kinetic theory (EKT) [72,73]. Despite differences in approach, these studies consistently conclude that the broadening per unit length in the short pre-equilibrium phase is considerably larger than in the equilibrated hydrophase.

In the present work, we extend our energy loss framework to the kinetic pre-equilibrium stage as follows. The out-of-equilibrium evolution of the local energy density has been extensively studied in EKT [74–79], and it is well captured by the hydrodynamic attractor. We use the attractor to extrapolate the effective local temperature for times τ earlier than $\tau_{\rm hyd}$ as [80,81]

$$(\tau^{1/3}T)^4_{\rm eff} = (\tau^{1/3}T)^4_{\rm hyd}\cdot\mathcal{E}(\tilde{\omega}), \tag{2}$$

where $\mathcal{E}(\tilde{\omega})$ is the attractor function, $\tilde{\omega} = \tau T_{\rm eff}/(4\pi\eta/s)$, and we implicitly used the the three flavor conformal equation of state of the EKT. We account for viscous corrections as

$$(\tau^{1/3}T)_{\rm hyd} = \tau_{\rm hyd}^{1/3}\left(T(x) + \frac{2}{3}\frac{\eta/s}{\tau_{\rm hyd}}\right) \tag{3}$$

with $\eta/s = 0.12$, where $T(x)$ is the local initial temperature. We assume that our energy-loss model can be applied without any additional modification by using these extrapolated pre-equilibrium temperatures. Before $\tau_{\rm min}$, and for the glasma phase, no quenching is applied, and we take this time as the second parameter of our Bayesian inference.

Finally, fluid velocity fields also evolve during the kinetic pre-equilibrium phase, as initial spatial anisotropies begin to generate flow [67]. This nonequilibrium evolution is well approximated by the universal preflow extracted from EKT [82]. We incorporate it by scaling the transverse velocity linearly with time:

$$\begin{aligned} v_{{\rm eff},T}(\tau,\vec{x}) &= \frac{\tau}{\tau_{\rm hyd}}v_T(\tau_{\rm hyd},\vec{x}),\\ v_{{\rm eff},z}(\tau) &= \tanh\eta_s, \end{aligned} \tag{4}$$

where the longitudinal velocity scales with the space-time rapidity η_s.

III. RESULTS

We evaluate the quenched inclusive jet spectrum $\sigma^{AA\%}(p_T,\eta,\phi,R)$ for various collision systems and centralities. Our focus is on the simultaneous description of $R^{\rm jet}_{AA}$ and $v^{\rm jet}_n$ observables, which we evaluate using

$$\begin{aligned} R^{\rm jet}_{AA} &= \sigma^{AA\%}(p_T,R)/\sigma^{pp}(p_T,R),\\ v^{\rm jet}_n &= \frac{\int d\eta d\phi\cos(n(\phi-\Psi_n))\sigma^{AA\%}(p_T,\eta,\phi,R)}{\sigma^{AA}(p_T,R)}, \end{aligned} \tag{5}$$

where $\sigma(p_T,R) = \int d\eta d\phi\sigma(p_T,\eta,\phi,R)$ with the appropriate experimental cuts. We use the event plane method to compute $v^{\rm jet}_n$, following the procedure in the ATLAS measurement to which we compare our model [83].[2] We evaluate the hadron spectrum as

$$\sigma(p^h_T,\eta,\phi) = \sum_{i=q,g}\int_x^1\frac{{\rm d}z}{z}\sigma_i\left(\frac{p^h_T}{z},R,\eta,\phi\right)D^h_i\left(z,\mu^2_F\right), \tag{6}$$

where $x = 2p^h_T\cosh(\eta)/\sqrt{s}$, and we used the jet scale $\mu_F = p^h_T R/z$. We averaged over (u,d,s) FFs and neglected the others. This simple convolution neglects medium effects in fragmentation, and thus ignores, for example, the impact of the angular redistribution of particles due to broadening.

Our work resembles previous studies of R_{AA} and v_2 [68,69,84,86–99]. In contrast to these works, we focus on jets instead of hadrons, since jets are infrared and collinear safe, and have small nonperturbative corrections in vacuum [100–103]. We use state-of-the-art hydrodynamics and energy-loss formulas, including elastic energy loss as well as the effects of medium response. To our knowledge, this is the first model implementation of jet energy loss in the pre-equilibrium phase carried out in a physically well-motivated manner.

We employ Bayesian inference, implemented via the JETSCAPE/STAT toolkit [104–106], to constrain the jet-medium strong coupling $g_{\rm med}$ and the initial quenching time in the pre-equilibrium phase $\tau_{\rm min}$. We used flat priors in the intervals $1.2 \leqslant g_{\rm med} \leqslant 1.7$ and $0.01 \leqslant \tau_{\rm min}\,[{\rm fm}] \leqslant 0.4$. We do not consider the scenario when $\tau_{\rm min} > \tau_{\rm hyd}$ as we believe delaying quenching beyond hydrodynamics is unphysical. Our data points include $R^{\rm jet}_{AA}$ at LHC energies for different jet cones and centrality selections [107–109], as well as jet $v^{\rm jet}_2$ [83], up to 40–50 % centrality. The inference incorporates statistical and systematic uncertainties of the data, and we estimate the full correlation matrix by employing a finite correlation length of 0.2 [105,110]. Luminosity and centrality uncertainties are added to the systematics. We neglect inherent model uncertainties in the inference such as scale and nPDF uncertainties, and we will present them separately for the OO predictions.

Figure 1 shows the parameter posterior for two different scenarios. Fitting only $R^{\rm jet}_{AA}$ (blue) results in little constraint on $\tau_{\rm min}$. This is expected, as an earlier starting time can be compensated by a relatively smaller medium coupling to produce the same energy loss. Including $v^{\rm jet}_2$ constrains $\tau_{\rm min} \approx 0.24$

[2] We also compared our results using the event plane method against the more experimentally common scalar product method, in which one correlates the jet momenta with the soft sector (see, e.g., [84]), and found very little change in v_2, below 4%, consistent with what was shown by ATLAS [85].

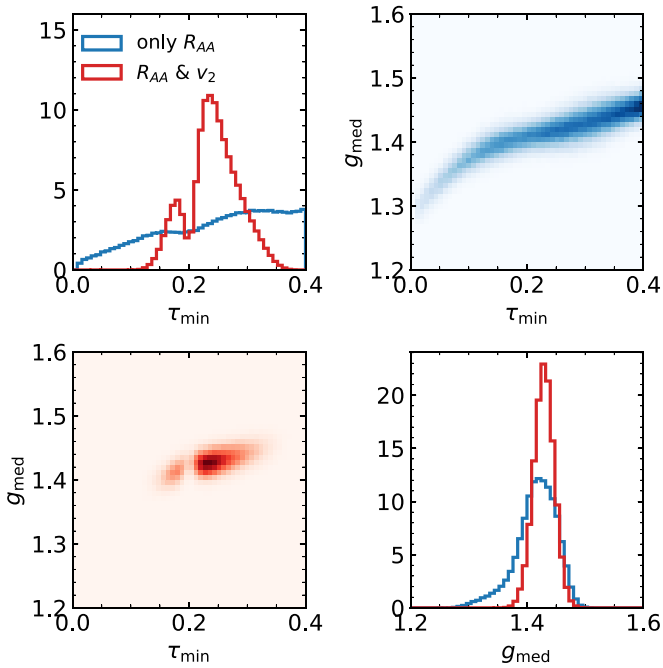


FIG. 1. Parameter posterior probability distributions and correlations. Red distributions include $R_{AA}^{\rm jet}$ and $v_2^{\rm jet}$ data, while blue only includes $R_{AA}^{\rm jet}$.

fm (red). This inference illustrates the role of pre-equilibrium effects in $v_2^{\rm jet}$.[3]

Before moving to our predictions for oxygen collisions, Figs. 4 and 5 in Appendix A show the posterior predictive distributions. We observe excellent overall agreement with all data. Small tensions can be found in $v_2^{\rm jet}$ at low p_T, which motivates further improvements of the energy loss framework. For completeness, Figs. 4 and 5 in Appendix A also show two additional inference results on $g_{\rm med}$ with two limiting scenarios: early pre-equilibrium with fixed $\tau_{\rm min} = 0.08$ fm, and no pre-equilibrium with $\tau_{\rm min} = 0.4$ fm. The best fit (whose parameters are shown in Fig. 1) outperforms these two scenarios, although differences are not very significant. The extracted bare jet transport coefficient is approximately $\hat{q}_0/T^3 \approx 1.7$, while after logarithmic corrections the effective value is $\hat{q}/T^3 = \hat{q}_0/T^3 \log(Q_s^2/\mu_*^2) \approx 7$, where $Q_s^2 = \hat{q}_0 L$, and $\mu_*^2 = m_D^2 e^{-2+2\gamma_E}/4$. We note that this extracted $\hat{q}$ is consistent with other recent extractions using Bayesian inference in the JETSCAPE framework [106].

Figures 6 and 7 in Appendix A provide predictions for jets at RHIC energies [111] and charged hadrons at LHC energies [85,112–114] using the extracted parameters. Even though our framework was designed for jets, it also provides a good description of the charged hadron R_{AA} without including them in the inference. We also see, however, that our framework underestimates hadron elliptic flow at low p_T. This failure is consistent with previous findings using pQCD energy loss [68,69]. It has been pointed out that a rather late quenching time of around ≈1 fm would resolve the disagreement [69]. Alternatively, the absence of this issue for jets signals the need for model improvements which could be more relevant for (mid-p_T) hadrons than for jets. Again, for completeness, we show predictions with the previous two limiting scenarios (early pre-equilibrium and no pre-equilibrium energy loss), resulting as before in subtle differences.

OO predictions. The recent OO run at the LHC has attracted considerable attention, with numerous dedicated studies on, for example, baseline analyses [115–118] and hadron quenching predictions [119–127]. Compared to these studies, our framework incorporates additional improvements, with an emphasis on jet observables. For our OO predictions of R_{AA} and v_2 we have set $\sqrt{s_{NN}} = 5.36$ TeV and $|\eta| < 2.1$. We defer to future work the computation of higher-order flow harmonics, along with the corresponding predictions for NeNe collisions.

Figure 2 shows our jet and charged hadron predictions for OO collisions. The left panel shows the inclusive jet suppression, where the no-quenching baseline, $\tilde{\sigma}^{pp}/\sigma^{pp}$, is indicated with gray bands. The dark band represents NLO scale uncertainties, while the light band is the 68% confidence of the nPDF. Below 50 GeV for jets and 30 GeV for hadrons, we underestimate nPDF uncertainties because of the relatively high momentum cutoff we chose for the NLO cross sections [117,118]. This cutoff does not affect the central value. Quenching effects are shown with red and blue for different centrality selections. Dark bands are the 68% confidence of our Bayesian parameter estimation, and on top of these, 68% nPDF uncertainties are shown with light bands. Peripheral collisions (30–100 %) are less suppressed than central ones (0–30 %), as expected, and clear quenching signals are present towards lower jet p_T for both centrality selections. The right panel in Fig. 2 shows the charged hadron suppression, which presents a similar pattern to jets.

Figure 3 shows the inclusive jet and charged hadron elliptic flow. There is relatively smaller sensitivity to the nPDF, as v_2 is an observable that is differential in the transverse plane, using solely the medium spectra, so the impact of the nPDF largely cancels in Eq. (5). Semi-inclusive observables can present analogous advantages [117]. We observe that, in contrast to large collision systems, the elliptic flow coefficient v_2 increases with centrality. This is a consequence of the more prominent role played by the fluctuations of the initial nuclear shape in small collision systems [119,121,128]. Jet distributions are not shown for very low p_T, where our framework is not expected to apply.

Due to the relatively small path lengths involved in OO, the typical value of the coherence angle is relatively large, $\theta_c \approx 0.5$, and so $R = 0.4$ jets are unresolved and lose energy as single color charges. Therefore, hadron and jet suppression in our framework can be understood by the mere p_T shift resulting from hadronization. In contrast, in larger systems (with smaller values of θ_c) both R_{AA} and v_2 receive additional contributions due to resolved jet substructure fluctuations [44,129].

Finally, Fig. 8 in Appendix B shows our OO predictions for minimum bias with the different limiting cases introduced

[3]It would be interesting to include $\tau_{\rm hyd}$ in the inference, since it could affect our results. This would require the simultaneous tuning of the soft and hard sectors, a task that we defer to future work.

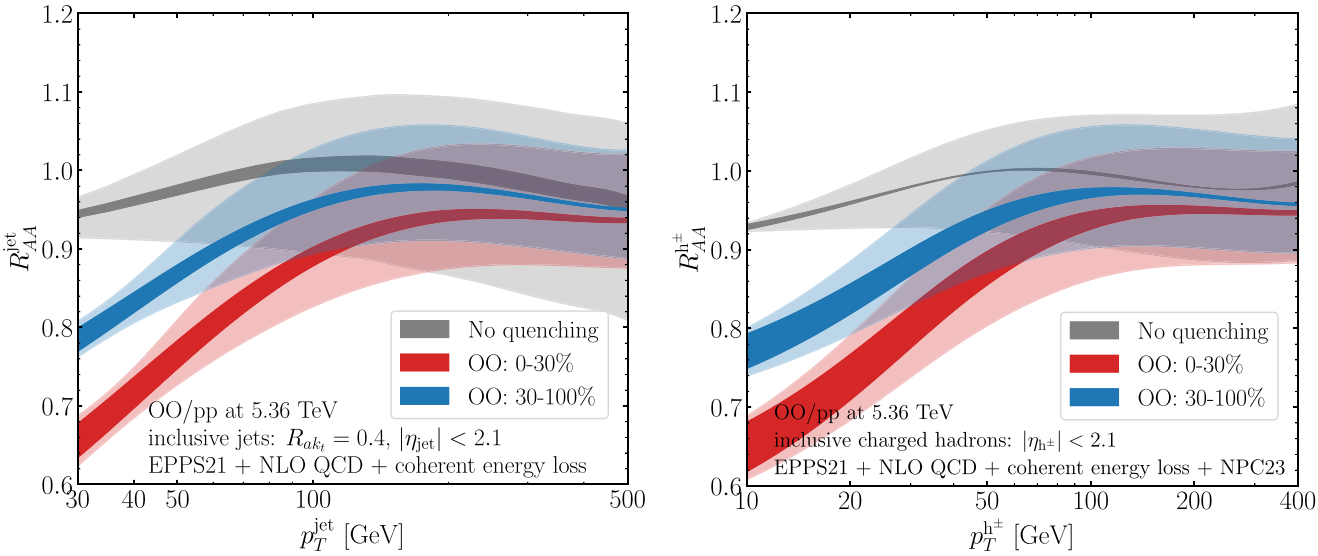


FIG. 2. Nuclear modification for jets and charged hadrons in OO collisions for two different centrality selections. Dark bands represent the 68% confidence interval for quenching parameters, and light bands represent the 68% nPDF uncertainties.

previously. Only subtle differences are observed for earlier vs later quenching for the ranges of $\tau_{\rm min}$ explored.

IV. CONCLUSIONS

In this work, we have integrated our semianalytical jet quenching model with a state-of-the-art description of heavy-ion collisions, IP-Glasma + JIMWLK + MUSIC + UrQMD. We incorporated energy loss in the pre-equilibrium phase via the hydrodynamic attractor for the first time. Our framework provides a simultaneous description of jet R_{AA} and v_2 in agreement with data in AA collisions, offering a strong validation of the approach. We show that a joint description of these observables places constraints on the onset time of jet-medium interactions, which is around 0.2 fm, deep in the pre-equilibrium phase. Then, we applied these parameters to predict jet and hadron quenching in other collision systems. We saw that our framework successfully predicts hadron suppression but underestimates hadron elliptic flow towards lower p_T. Our results provide a complementary perspective to previous phenomenological studies. By incorporating early-time energy loss, we achieve a simultaneous description of jet R_{AA} and v_2, as well as hadron R_{AA} and v_2 at high-p_T. This resolves, in our opinion, the unphysical delay of quenching invoked in earlier approaches (e.g., [68,69]) to reproduce hadron R_{AA} and v_2. The successful description of jet observables supports the onset of quenching at early times, whereas the

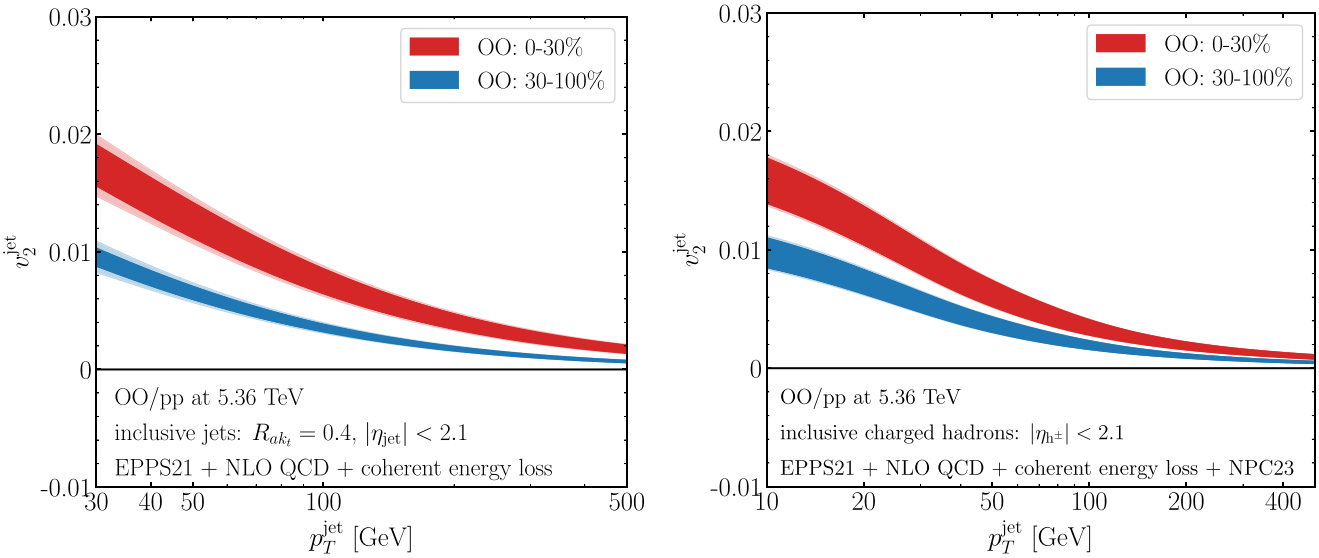


FIG. 3. Charged hadron and jet elliptic flow in oxygen collisions for two different centrality selections. Dark bands represent the 68% confidence interval for quenching parameters, while light bands represent the 68% nPDF uncertainties.

remaining discrepancy in hadron v_2 at moderate transverse momentum indicates the necessity of additional medium effects beyond longitudinal energy loss.

Our constrained framework has been used to make realistic predictions for the intermediate-sized OO collisions. We obtained sizable energy loss both for jets and charged hadrons, in quantitative agreement with the results from CMS [130], where our predictions are also presented. Even though we have shown that pre-equilibrium effects play a moderate role in our model, we anticipate that including forthcoming data on high-p_T flow coefficients will result in further constraints. Furthermore, in this work we have provided predictions for elliptic anisotropies and different centrality selections, both for hadrons and jets. Due to the small path lengths in OO, unlike in PbPb or AuAu, jet constituents are barely resolved (jets are fully coherent), and thus we obtain similar energy loss for hadrons and jets (modulo a p_T shift in fragmentation). This outcome constitutes a prediction of our framework which can be confronted with future experimental results on jet suppression in light ions. All of our data and plots are available at [131].

As an outlook, our jet quenching framework could benefit from an improved description of medium-induced emissions, elastic scatterings, and medium response in several ways. It is important to note that, at very early times, local color fields are saturated and highly anisotropic, a scenario which our energy-loss framework, built on local equilibrium, cannot accommodate. For these initial stages, it would be desirable to incorporate recent developments in energy-loss calculations for anisotropic and flowing media [132–138], correlated color fields [139], and out of-equilibrium plasma [140,141], so as to extend quenching for those earliest times where the attractor solution is not meant to apply.

ACKNOWLEDGMENTS

We are grateful to Björn Schenke and Chun Shen for sharing the hydrodynamic profiles and to Jannis Gebhard for sharing oxygen events. We greatly appreciate discussions with Aleksas Mazeliauskas, Yacine Mehtar-Tani, and Konrad Tywoniuk. The work of A.T. is supported by DFG through Emmy Noether Programme (Project No. 496831614) and through CRC 1225 ISOQUANT (Project No. 27381115). D.P. is funded by the European Union's Horizon 2020 research and innovation program under the Marie Sklodowska-Curie Grant Agreement No. 101155036 (AntScat), by the European Research Council Project No. ERC-2018-ADG-835105 YoctoLHC, by the Spanish Research State Agency under Project No. PID2020-119632GB-I00, by Xunta de Galicia (CIGUS Network of Research Centres) and the European Union, and by Unidad de Excelencia María de Maetzu under Project No. CEX2023-001318-M. D.P. also acknowledges support from the the Ramón y Cajal fellowship Grant No. RYC2023-044989-I.

DATA AVAILABILITY

The data that support the findings of this article are openly available [131], embargo periods may apply.

APPENDIX A: BAYESIAN PARAMETER ESTIMATION

We have already introduced our Bayesian framework in Sec. II, and here, we extend this discussion by providing additional details. In this appendix, PbPb and AuAu cross sections $\tilde{\sigma}^{AA}(p_T, \eta, R)$ are computed using the microjet evolution as employed in [42,44], with initial conditions from LO Pythia at $R_0 = 1$. Our framework is built on the JETSCAPE/STAT toolkit [104–106]. We evaluated our model for 24 design points, equally distributed in the parameter space. To focus on primary model features that are robust against statistical uncertainty, we reduced our data to its ten principal components, and trained a Gaussian process emulator to interpolate between the predictions. The resulting parameter posterior is shown in the main text in Fig. 1. Furthermore, we provide two alternative inferences for $g_{\rm med}$: one with fixed $\tau_{\rm min} = 0.08$ fm, (and extracted $\langle g_{\rm med}\rangle = 1.385$) referred to as "early preeq", and another with $\tau_{\rm min} = 0.4$ fm, (extracted $\langle g_{\rm med}\rangle = 1.473$), referred to as "no preeq".

Figures 4 and 5 show the corresponding posterior predictive distributions. These jet data were used to constrain the model parameters. Different rows correspond to different measurements. We observe good agreement with all data for both $R_{AA}^{\rm jet}$ and $v_2^{\rm jet}$, including all collision energies, centralities, rapidities, jet cone sizes, and momenta. There is a slight tension in $v_2^{\rm jet}$ for the lowest p_T bins. This tension could be do to missing ingredients in the description of energy loss towards lower p_T. Dotted and dashed lines show the two alternative fits, where $\tau_{\rm min}$ is kept fixed. There are subtle differences between different fits, with the fixed earlier quenching reducing the jet v_2, as expected. Finally, we also compare our results to jets at RHIC energies and charged hadron observables, shown in Figs. 6 and 7. As our framework was designed for jets, we did not include these data in the inference. We see an overall good agreement with both RHIC energies and charged hadron R_{AA}. Interestingly, hadron R_{AA} seems to favor early quenching, as indicated by the dashed lines. There is a clear underestimation of the hadron elliptic flow at low momenta, consistent with previous findings from other theory collaborations, likely linked to the (milder) tension with low p_T jets mentioned above.

APPENDIX B: OO PREDICTIONS WITHOUT PRE-EQUILIBRIUM QUENCHING

Figure 8 shows the nuclear modification and elliptic flow for minimum bias OO collisions. Curves represent the limiting scenarios tested in Appendix A regarding pre-equilibrium quenching: "early preeq" denotes $\tau_{\rm min} = 0.08$ fm, "no preeq" $\tau_{\rm min} = 0.4$ fm, with their corresponding inferred $g_{\rm med}$. The best fit denotes our default setting shown in Fig. 1. For simplicity, we do not show nPDF uncertainties. Slight differences are present in the different limiting scenarios. Interestingly, an earlier quenching can result in a relatively larger v_2, in contrast to larger systems, likely reflecting the more important role of fluctuations over average geometry in smaller systems.

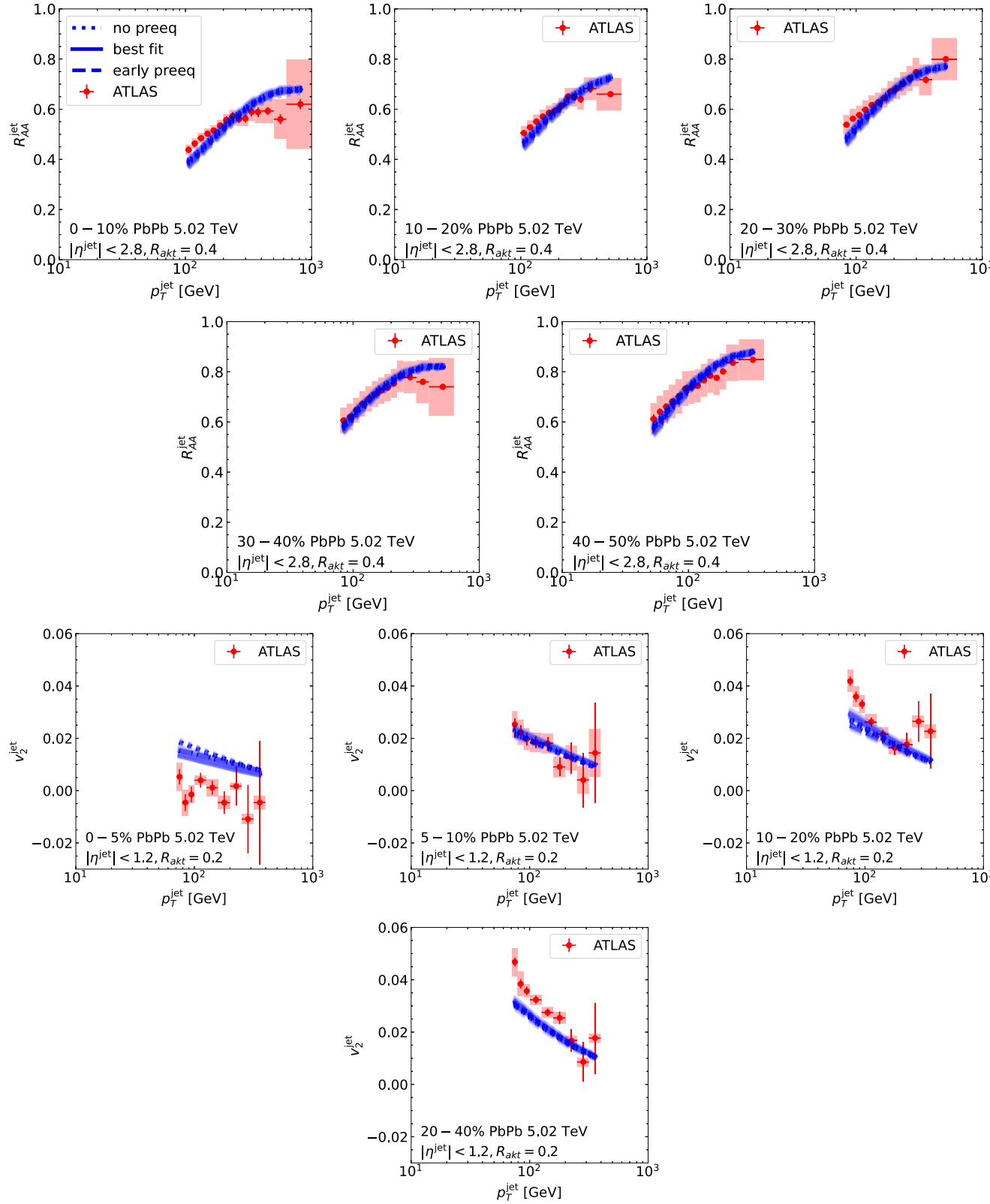


FIG. 4. Posterior predictive distributions, the fitting performance of our model. Jet R_{AA} and jet v_2 data from ATLAS.

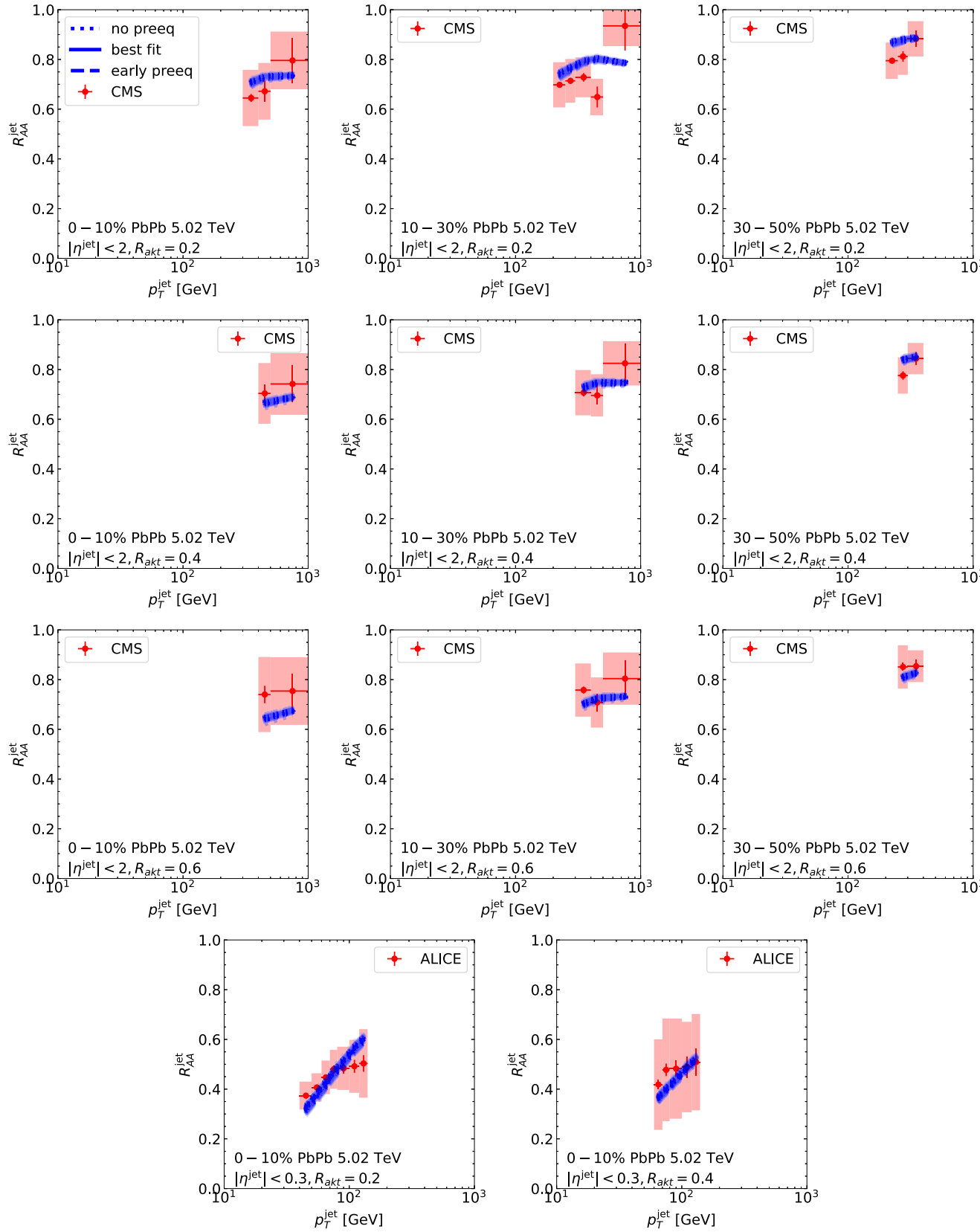


FIG. 5. Posterior predictive distributions, the fitting performance of our model. Jet R_{AA} from ALICE and CMS.

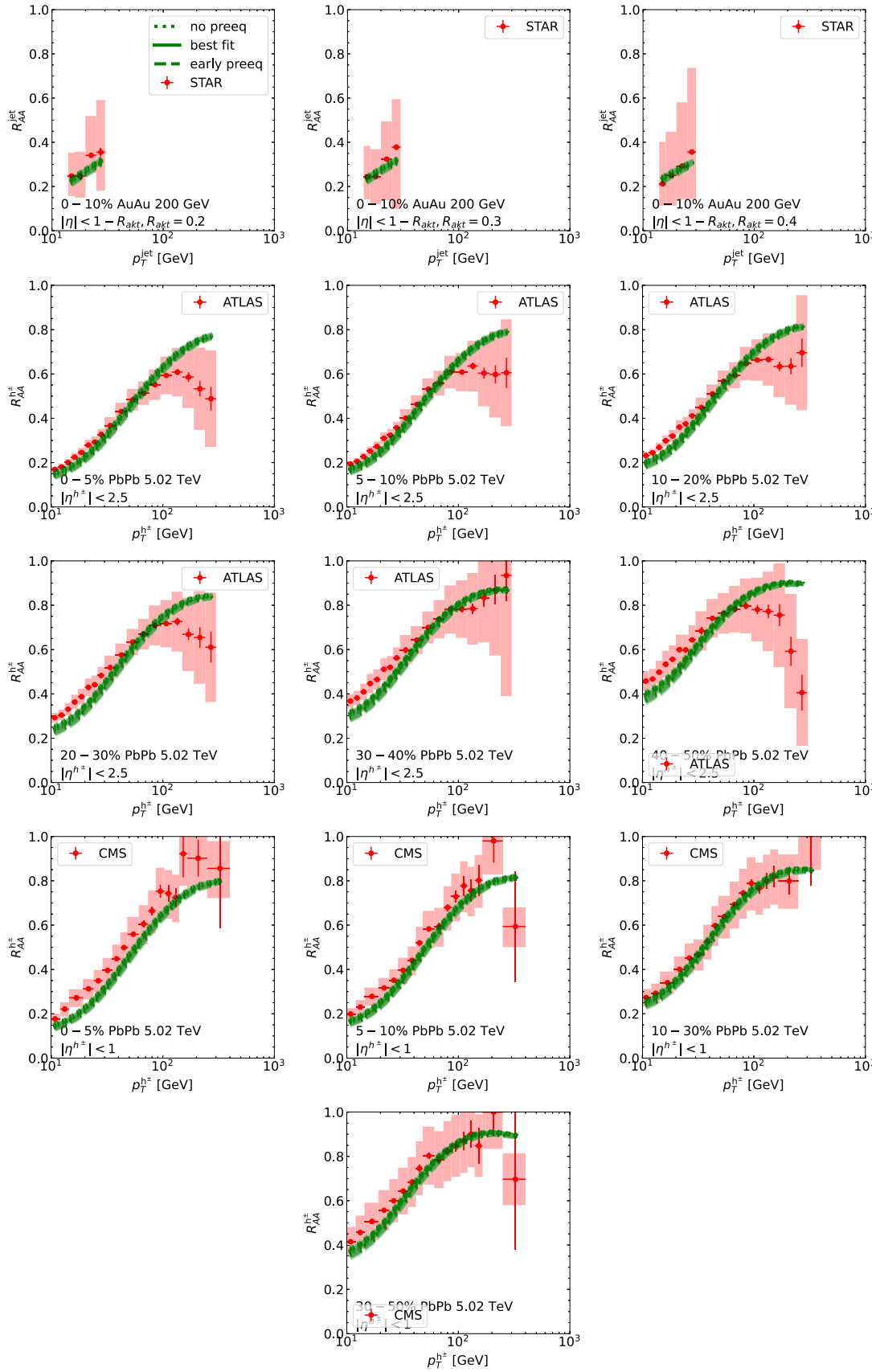


FIG. 6. Posterior predictive distributions for RHIC energy and for hadrons (not included in the inference). Data shown for RHIC jets and charged hadrons across different LHC experiments.

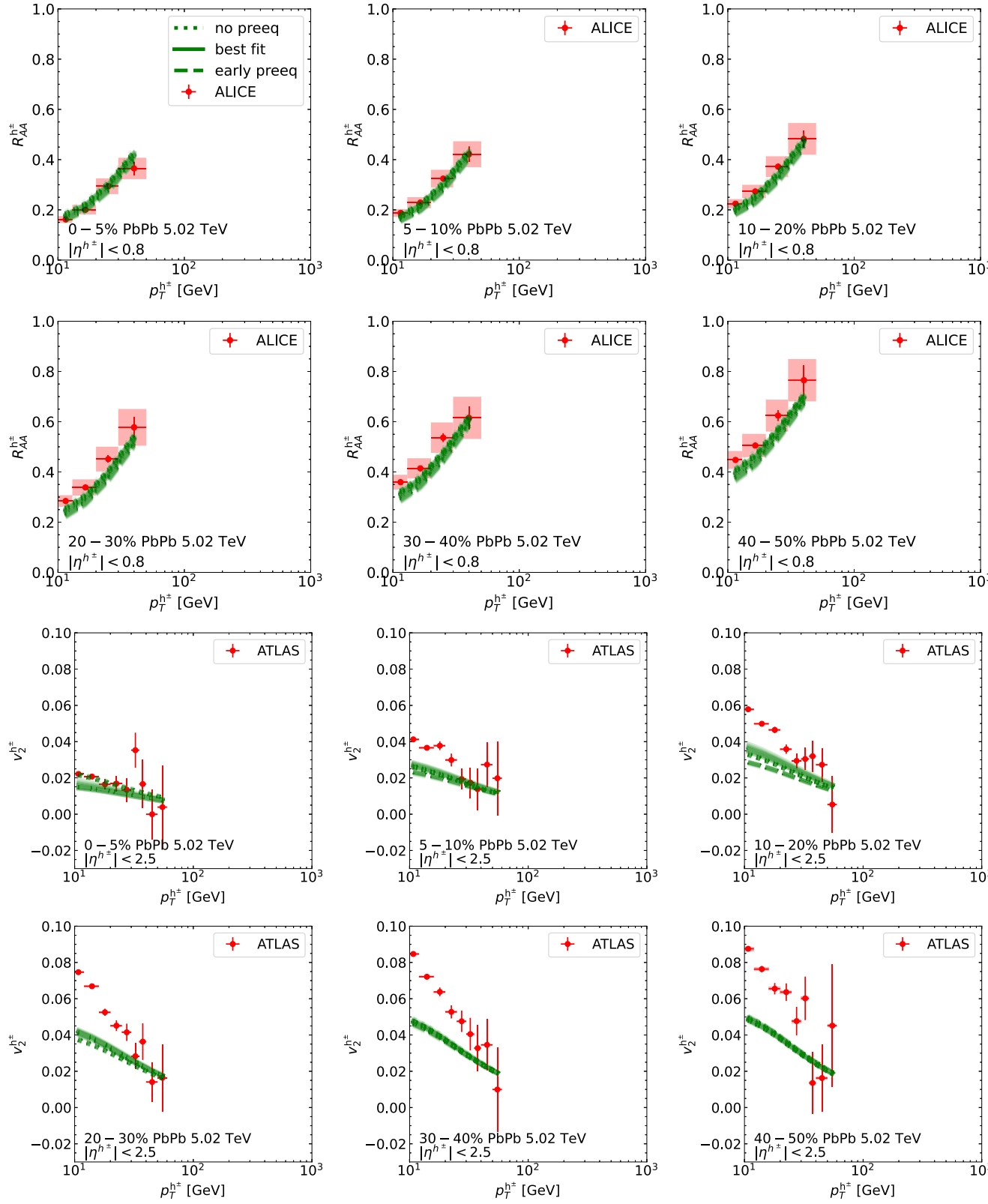


FIG. 7. Posterior predictive distributions for RHIC energy and for hadrons (not included in the inference). Data shown for RHIC jets and charged hadrons across different LHC experiments.

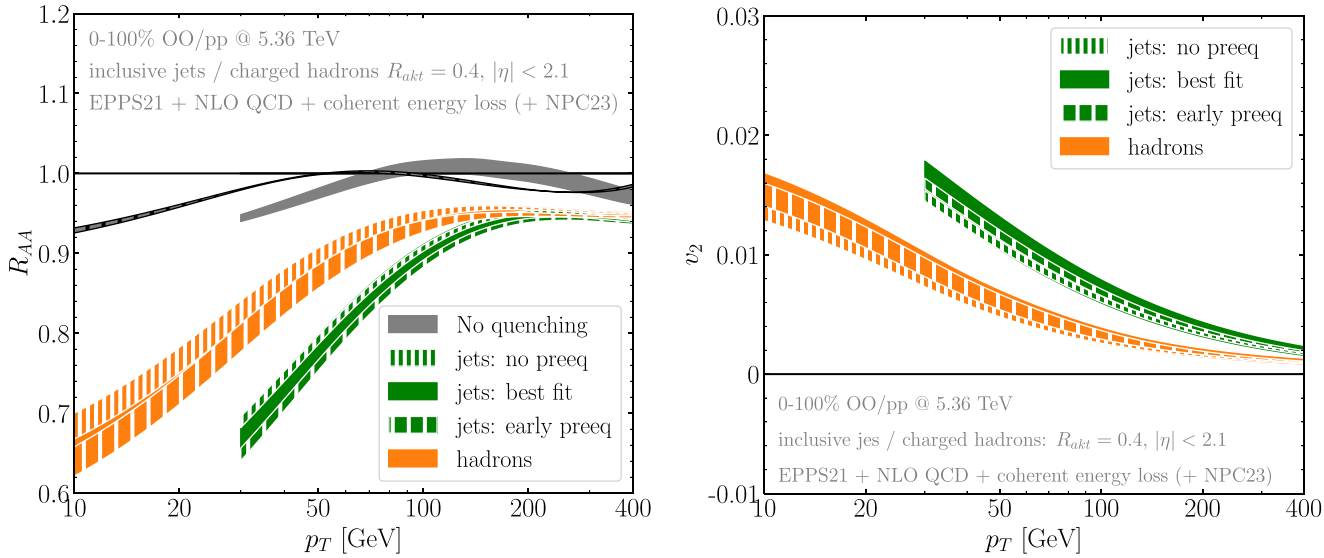


FIG. 8. Nuclear modification and elliptic flow for jets and charged hadrons in minimum bias OO collisions. Different lines corresponds to different limiting scenarios in the pre-equilibrium quenching. The bands represent the 68% confidence interval for quenching parameters.

[1] V. Khachatryan *et al.* (CMS Collaobration), Observation of long-range near-side angular correlations in proton-proton collisions at the LHC, J. High Energy Phys. 09 (2021) 091.

[2] G. Aad *et al.* (ATLAS Collaboration), Observation of associated near-side and away-side long-range correlations in $\sqrt{s_{NN}}$=5.02 TeV proton-lead collisions with the ATLAS detector, Phys. Rev. Lett. **110**, 182302 (2013).

[3] B. Abelev *et al.* (ALICE Collaboration), Long-range angular correlations on the near and away side in *p*-Pb collisions at $\sqrt{s_{NN}} = 5.02$ TeV, Phys. Lett. B **719**, 29 (2013).

[4] S. C. Junior *et al.* (CMS Collaboration), Observation of long-range near-side angular correlations in proton-lead collisions at the LHC, Phys. Lett. B **718**, 795 (2013).

[5] J. L. Nagle and W. A. Zajc, Small system collectivity in relativistic hadronic and nuclear collisions, Annu. Rev. Nucl. Part. Sci. **68**, 211 (2018).

[6] J. Noronha, B. Schenke, C. Shen, and W. Zhao, Progress and challenges in small systems, Int. J. Mod. Phys. E **33**, 2430005 (2024).

[7] J. F. Grosse-Oetringhaus and U. A. Wiedemann, A decade of collectivity in small systems, arXiv:2407.07484.

[8] R. D. Weller and P. Romatschke, One fluid to rule them all: viscous hydrodynamic description of event-by-event central p+p, p+Pb and Pb+Pb collisions at $\sqrt{s} = 5.02$ TeV, Phys. Lett. B **774**, 351 (2017).

[9] C. Aidala *et al.* (PHENIX Collaboration), Creation of quark-gluon plasma droplets with three distinct geometries, Nat. Phys. **15**, 214 (2019).

[10] S. Acharya *et al.* (ALICE Collaboration), Investigations of anisotropic flow using multiparticle azimuthal correlations in pp, p-Pb, Xe-Xe, and Pb-Pb collisions at the LHC, Phys. Rev. Lett. **123**, 142301 (2019).

[11] G. Nijs, W. van der Schee, U. Gürsoy, and R. Snellings, Bayesian analysis of heavy ion collisions with the heavy ion computational framework TRAJECTUM, Phys. Rev. C **103**, 054909 (2021).

[12] C. Bierlich, G. Gustafson, L. Lönnblad, and H. Shah, The Angantyr model for heavy-ion collisions in PYTHIA8, J. High Energy Phys. 10 (2018) 134.

[13] A. Kurkela, A. Mazeliauskas, and R. Törnkvist, Collective flow in single-hit QCD kinetic theory, J. High Energy Phys. 11 (2021) 216.

[14] C. Bierlich, P. Christiansen, G. Gustafson, L. Lönnblad, R. Törnkvist, and K. Zapp, Going against the flow: Revealing the QCD degrees of freedom in hadronic collisions, arXiv:2409.16093.

[15] M. S. Torres, Y. Feng, and F. Wang, Azimuthal correlation anisotropies in $p + p$ collisions simulated by PYTHIA, Chinese Phys. C **49**, 044001 (2025).

[16] I. Soudi and A. Majumder, T-odd parton distribution functions and azimuthal anisotropy at high transverse momentum in p-p and p-A collisions, Phys. Rev. C **111**, 024901 (2025).

[17] I. Soudi *et al.* (JETSCAPE Collaboration), Soft-hard framework with exact four-momentum conservation for small systems, Phys. Rev. C **112**, 014905 (2025).

[18] N. Armesto and E. Scomparin, Heavy-ion collisions at the Large Hadron Collider: a review of the results from Run 1, Eur. Phys. J. Plus **131**, 52 (2016).

[19] M. Connors, C. Nattrass, R. Reed, and S. Salur, Jet measurements in heavy ion physics, Rev. Mod. Phys. **90**, 025005 (2018).

[20] L. Cunqueiro and A. M. Sickles, Studying the QGP with jets at the LHC and RHIC, Prog. Part. Nucl. Phys. **124**, 103940 (2022).

[21] J. Casalderrey-Solana and C. A. Salgado, Introductory lectures on jet quenching in heavy ion collisions, Acta Phys. Pol. B **38**, 3731 (2007).

[22] D. d'Enterria, Jet quenching, Landolt-Bornstein **23**, 471 (2010).

[23] Y. Mehtar-tani, J. G. Milhano, and K. Tywoniuk, Jet physics in heavy-ion collisions, Int. J. Mod. Phys. A **28**, 1340013 (2013).

[24] S. Cao, A. Majumder, R. Modarresi-Yazdi, I. Soudi, and Y. Tachibana, Jet quenching: From theory to simulation, Int. J. Mod. Phys. E **33**, 2430002 (2024).

[25] G. Aad *et al.* (ATLAS Collaboration), Centrality and rapidity dependence of inclusive jet production in $\sqrt{s_{\rm NN}} = 5.02$ TeV proton-lead collisions with the ATLAS detector, Phys. Lett. B **748**, 392 (2015).

[26] J. Adam *et al.* (ALICE Collaboration), Centrality dependence of charged jet production in p-Pb collisions at $\sqrt{s_{\rm NN}} = 5.02$ TeV, Eur. Phys. J. C **76**, 271 (2016).

[27] S. Acharya *et al.* (ALICE Collaboration), Measurement of inclusive charged-particle b-jet production in pp and p-Pb collisions at $\sqrt{s_{\rm NN}} = 5.02$ TeV, J. High Energy Phys. 01 (2022) 178.

[28] S. Acharya *et al.* (ALICE Collaboration), Measurement of inclusive charged-particle jet production in pp and p-Pb collisions at $\sqrt{s_{\rm NN}} = 5.02$ TeV, J. High Energy Phys. 05 (2024) 041.

[29] G. Aad *et al.* (ATLAS Collaboration), Transverse momentum and process dependent azimuthal anisotropies in $\sqrt{s_{\rm NN}} = 8.16$TeV $p+$Pb collisions with the ATLAS detector, Eur. Phys. J. C **80**, 73 (2020).

[30] G. Aad *et al.* (ATLAS Collaboration), Measurement of the sensitivity of two-particle correlations in pp collisions to the presence of hard scatterings, Phys. Rev. Lett. **131**, 162301 (2023).

[31] V. Chekhovsky *et al.* (CMS Collaboration), Evidence for similar collectivity of high transverse momentum particles in p-Pb and Pb-Pb collisions, Phys. Rev. Lett. **135**, 071903 (2025).

[32] M. Gyulassy, I. Vitev, and X. N. Wang, High p_T azimuthal asymmetry in noncentral $A + A$ at RHIC, Phys. Rev. Lett. **86**, 2537 (2001).

[33] X.-N. Wang, Jet quenching and azimuthal anisotropy of large p_T spectra in noncentral high-energy heavy ion collisions, Phys. Rev. C **63**, 054902 (2001).

[34] Z. Citron *et al.*, Report from Working Group 5: Future physics opportunities for high-density QCD at the LHC with heavy-ion and proton beams, CERN Yellow Rep. Monogr. **7**, 1159 (2019).

[35] J. Brewer, A. Mazeliauskas, and W. van der Schee, Opportunities of OO and pO collisions at the LHC, arXiv:2103.01939.

[36] C. Loizides and A. Morsch, Absence of jet quenching in peripheral nucleus–nucleus collisions, Phys. Lett. B **773**, 408 (2017).

[37] J. Park, J. L. Nagle, D. V. Perepelitsa, S. Lim, and C. Loizides, Selection bias effects on high-$p_{\rm T}$ yield and correlation measurements in oxygen+oxygen collisions, Phys. Rev. C **112**, 064916 (2025).

[38] U. Heinz and R. Snellings, Collective flow and viscosity in relativistic heavy-ion collisions, Annu. Rev. Nucl. Part. Sci. **63**, 123 (2013).

[39] C. Gale, S. Jeon, and B. Schenke, Hydrodynamic modeling of heavy-ion collisions, Int. J. Mod. Phys. A **28**, 1340011 (2013).

[40] H. Mäntysaari, B. Schenke, C. Shen, and P. Tribedy, Imprints of fluctuating proton shapes on flow in proton-lead collisions at the LHC, Phys. Lett. B **772**, 681 (2017).

[41] P. Romatschke and U. Romatschke, *Relativistic Fluid Dynamics In and Out of Equilibrium*, Cambridge Monographs on Mathematical Physics (Cambridge University Press, Cambridge, 2019).

[42] Y. Mehtar-Tani, D. Pablos, and K. Tywoniuk, Cone-size dependence of jet suppression in heavy-ion collisions, Phys. Rev. Lett. **127**, 252301 (2021).

[43] A. Takacs and K. Tywoniuk, Quenching effects in the cumulative jet spectrum, J. High Energy Phys. 10 (2021) 038.

[44] Y. Mehtar-Tani, D. Pablos, and K. Tywoniuk, Jet suppression and azimuthal anisotropy from RHIC to LHC, Phys. Rev. D **110**, 014009 (2024).

[45] J. Alwall, R. Frederix, S. Frixione, V. Hirschi, F. Maltoni, O. Mattelaer, H. S. Shao, T. Stelzer, P. Torrielli, and M. Zaro, The automated computation of tree-level and next-to-leading order differential cross sections, and their matching to parton shower simulations, J. High Energy Phys. 07 (2014) 079.

[46] C. Bierlich *et al.*, A comprehensive guide to the physics and usage of PYTHIA 8.3, SciPost Phys. Codebases **2022**, 8 (2022).

[47] P. Skands, S. Carrazza, and J. Rojo, Tuning PYTHIA 8.1: the Monash 2013 Tune, Eur. Phys. J. C **74**, 3024 (2014).

[48] A. Banfi, G. P. Salam, and G. Zanderighi, Infrared safe definition of jet flavor, Eur. Phys. J. C **47**, 113 (2006).

[49] K. J. Eskola, P. Paakkinen, H. Paukkunen, and C. A. Salgado, EPPS21: A global QCD analysis of nuclear PDFs, Eur. Phys. J. C **82**, 413 (2022).

[50] A. Buckley, J. Ferrando, S. Lloyd, K. Nordström, B. Page, M. Rüfenacht, M. Schönherr, and G. Watt, LHAPDF6: Parton density access in the LHC precision era, Eur. Phys. J. C **75**, 132 (2015).

[51] J. Gao, C. Liu, X. Shen, H. Xing, and Y. Zhao, Global analysis of fragmentation functions to charged hadrons with high-precision data from the LHC, Phys. Rev. D **110**, 114019 (2024).

[52] Y. Mehtar-Tani, Gluon bremsstrahlung in finite media beyond multiple soft scattering approximation, J. High Energy Phys. 07 (2019) 057.

[53] J. a. Barata, Y. Mehtar-Tani, A. Soto-Ontoso, and K. Tywoniuk, Revisiting transverse momentum broadening in dense QCD media, Phys. Rev. D **104**, 054047 (2021).

[54] S. P. Adhya, C. A. Salgado, M. Spousta, and K. Tywoniuk, Medium-induced cascade in expanding media, J. High Energy Phys. 07 (2020) 150.

[55] P. Caucal, E. Iancu, A. H. Mueller, and G. Soyez, Nuclear modification factors for jet fragmentation, J. High Energy Phys. 10 (2020) 204.

[56] J.-P. Blaizot and Y. Mehtar-Tani, Jet structure in heavy ion collisions, Int. J. Mod. Phys. E **24**, 1530012 (2015).

[57] J. Casalderrey-Solana, E. V. Shuryak, and D. Teaney, Conical flow induced by quenched QCD jets, J. Phys.: Conf. Ser. **27**, 22 (2005).

[58] P. M. Chesler and L. G. Yaffe, The Wake of a quark moving through a strongly-coupled plasma, Phys. Rev. Lett. **99**, 152001 (2007).

[59] P. Caucal, E. Iancu, A. H. Mueller, and G. Soyez, Vacuum-like jet fragmentation in a dense QCD medium, Phys. Rev. Lett. **120**, 232001 (2018).

[60] Y. Mehtar-Tani and K. Tywoniuk, Sudakov suppression of jets in QCD media, Phys. Rev. D **98**, 051501 (2018).

[61] Y. Mehtar-Tani, C. A. Salgado, and K. Tywoniuk, Anti-angular ordering of gluon radiation in QCD media, Phys. Rev. Lett. **106**, 122002 (2011).

[62] Y. Mehtar-Tani, C. A. Salgado, and K. Tywoniuk, Jets in QCD media: From color coherence to decoherence, Phys. Lett. B **707**, 156 (2012).

[63] J. Casalderrey-Solana and E. Iancu, Interference effects in medium-induced gluon radiation, J. High Energy Phys. 08 (2011) 015.

[64] H. Mäntysaari, B. Schenke, C. Shen, and W. Zhao, Collision-energy dependence in heavy-ion collisions from nonlinear QCD evolution, Phys. Rev. Lett. **135**, 022302 (2025).

[65] H. Kowalski and D. Teaney, An Impact parameter dipole saturation model, Phys. Rev. D **68**, 114005 (2003).

[66] S. Schlichting and D. Teaney, The first fm/c of heavy-ion collisions, Annu. Rev. Nucl. Part. Sci. **69**, 447 (2019).

[67] J. Berges, M. P. Heller, A. Mazeliauskas, and R. Venugopalan, QCD thermalization: *ab initio* approaches and interdisciplinary connections, Rev. Mod. Phys. **93**, 035003 (2021).

[68] C. Andres, N. Armesto, H. Niemi, R. Paatelainen, and C. A. Salgado, Jet quenching as a probe of the initial stages in heavy-ion collisions, Phys. Lett. B **803**, 135318 (2020).

[69] S. Stojku, J. Auvinen, M. Djordjevic, P. Huovinen, and M. Djordjevic, Early evolution constrained by high-p ⊥ quark-gluon plasma tomography, Phys. Rev. C **105**, L021901 (2022).

[70] A. Ipp, D. I. Müller, and D. Schuh, Jet momentum broadening in the pre-equilibrium glasma, Phys. Lett. B **810**, 135810 (2020).

[71] D. Avramescu, V. Băran, V. Greco, A. Ipp, D. I. Müller, and M. Ruggieri, Simulating jets and heavy quarks in the glasma using the colored particle-in-cell method, Phys. Rev. D **107**, 114021 (2023).

[72] K. Boguslavski, A. Kurkela, T. Lappi, F. Lindenbauer, and J. Peuron, Jet momentum broadening during initial stages in heavy-ion collisions, Phys. Lett. B **850**, 138525 (2024).

[73] K. Boguslavski, A. Kurkela, T. Lappi, F. Lindenbauer, and J. Peuron, Jet quenching parameter in QCD kinetic theory, Phys. Rev. D **110**, 034019 (2024).

[74] A. Kurkela, A. Mazeliauskas, J.-F. Paquet, S. Schlichting, and D. Teaney, Matching the nonequilibrium initial stage of heavy ion collisions to hydrodynamics with QCD kinetic theory, Phys. Rev. Lett. **122**, 122302 (2019).

[75] A. Kurkela, A. Mazeliauskas, J.-F. Paquet, S. Schlichting, and D. Teaney, Effective kinetic description of event-by-event pre-equilibrium dynamics in high-energy heavy-ion collisions, Phys. Rev. C **99**, 034910 (2019).

[76] A. Mazeliauskas and J. Berges, Prescaling and far-from-equilibrium hydrodynamics in the quark-gluon plasma, Phys. Rev. Lett. **122**, 122301 (2019).

[77] A. Kurkela, W. van der Schee, U. A. Wiedemann, and B. Wu, Early- and late-time behavior of attractors in heavy-ion collisions, Phys. Rev. Lett. **124**, 102301 (2020).

[78] D. Almaalol, A. Kurkela, and M. Strickland, Nonequilibrium attractor in high-temperature QCD plasmas, Phys. Rev. Lett. **125**, 122302 (2020).

[79] A. Soloviev, Hydrodynamic attractors in heavy ion collisions: a review, Eur. Phys. J. C **82**, 319 (2022).

[80] G. Giacalone, A. Mazeliauskas, and S. Schlichting, Hydrodynamic attractors, initial state energy and particle production in relativistic nuclear collisions, Phys. Rev. Lett. **123**, 262301 (2019).

[81] O. Garcia-Montero, A. Mazeliauskas, P. Plaschke, and S. Schlichting, Pre-equilibrium photons from the early stages of heavy-ion collisions, J. High Energy Phys. 03 (2024) 053.

[82] L. Keegan, A. Kurkela, A. Mazeliauskas, and D. Teaney, Initial conditions for hydrodynamics from weakly coupled pre-equilibrium evolution, J. High Energy Phys. 08 (2016) 171.

[83] G. Aad *et al.* (ATLAS Collaboration), Measurements of azimuthal anisotropies of jet production in Pb+Pb collisions at $\sqrt{s_{NN}} = 5.02$ TeV with the ATLAS detector, Phys. Rev. C **105**, 064903 (2022).

[84] J. Noronha-Hostler, B. Betz, J. Noronha, and M. Gyulassy, Event-by-event hydrodynamics + jet energy loss: A solution to the $R_{AA} \otimes v_2$ puzzle, Phys. Rev. Lett. **116**, 252301 (2016).

[85] M. Aaboud, Jr. *et al.* (ATLAS Collaboration), Measurement of the azimuthal anisotropy of charged particles produced in $\sqrt{s_{\rm NN}} = 5.02$ TeV Pb+Pb collisions with the ATLAS detector, Eur. Phys. J. C **78**, 997 (2018).

[86] B. Betz and M. Gyulassy, Constraints on the path-length dependence of jet quenching in nuclear collisions at RHIC and LHC, J. High Energy Phys. 08 (2014) 090; 10 (2014) 043.

[87] C. Andres, L. Apolinário, F. Dominguez, M. G. Martinez, and C. A. Salgado, Medium-induced radiation with vacuum propagation in the pre-hydrodynamics phase, J. High Energy Phys. 03 (2023) 189.

[88] F. Arleo and G. Falmagne, Probing the path-length dependence of parton energy loss via scaling properties in heavy ion collisions, Phys. Rev. D **109**, L051503 (2024).

[89] C. Faraday and W. A. Horowitz, A unified description of small, peripheral, and large system suppression data from pQCD, Phys. Lett. B **864**, 139437 (2025).

[90] D. Zigic, I. Salom, J. Auvinen, M. Djordjevic, and M. Djordjevic, DREENA-C framework: joint R_{AA} and v_2 predictions and implications to QGP tomography, J. Phys. G **46**, 085101 (2019).

[91] D. Zigic, I. Salom, J. Auvinen, M. Djordjevic, and M. Djordjevic, DREENA-B framework: First predictions of R_{AA} and v_2 within dynamical energy loss formalism in evolving QCD medium, Phys. Lett. B **791**, 236 (2019).

[92] D. Zigic, B. Ilic, M. Djordjevic, and M. Djordjevic, Exploring the initial stages in heavy-ion collisions with high-$p_\perp R_{AA}$ and v_2 theory and data, Phys. Rev. C **101**, 064909 (2020).

[93] D. Zigic, I. Salom, J. Auvinen, P. Huovinen, and M. Djordjevic, DREENA-A framework as a QGP tomography tool, Front. Phys. **10**, 957019 (2022).

[94] D. Zigic, J. Auvinen, I. Salom, M. Djordjevic, and P. Huovinen, Importance of higher harmonics and v_4 puzzle in quark-gluon plasma tomography, Phys. Rev. C **106**, 044909 (2022).

[95] B. Karmakar, D. Zigic, I. Salom, J. Auvinen, P. Huovinen, M. Djordjevic, and M. Djordjevic, Constraining η/s through high-p ⊥ theory and data, Phys. Rev. C **108**, 044907 (2023).

[96] B. Karmakar, D. Zigic, M. Djordjevic, P. Huovinen, M. Djordjevic, and J. Auvinen, Probing the shape of the quark-gluon plasma droplet via event-by-event quark-gluon plasma tomography, Phys. Rev. C **110**, 044906 (2024).

[97] W. Zhao, W. Ke, W. Chen, T. Luo, and X.-N. Wang, From hydrodynamics to jet quenching, coalescence, and hadron cascade: A coupled approach to solving the $R_{AA} \otimes v_2$ puzzle, Phys. Rev. Lett. **128**, 022302 (2022).

[98] L. Barreto, F. M. Canedo, M. G. Munhoz, J. Noronha, and J. Noronha-Hostler, Jet cone radius dependence of R_{AA} and v_2 at PbPb 5.02 TeV from JEWEL+T$_R$ENTo+v-USPhydro, Phys. Lett. B **860**, 139217 (2025).

[99] Y. He, W. Chen, T. Luo, S. Cao, L.-G. Pang, and X.-N. Wang, Event-by-event jet anisotropy and hard-soft tomography of the quark-gluon plasma, Phys. Rev. C **106**, 044904 (2022).

[100] R. K. Ellis, W. J. Stirling, and B. R. Webber, *QCD and Collider Physics*, Cambridge Monographs on Particle Physics, Nuclear Physics, and Cosmology (Cambridge University Press, Cambridge, 2003).

[101] G. P. Salam, Elements of QCD for Hadron Colliders, arXiv:1011.5131.

[102] G. Luisoni and S. Marzani, QCD resummation for hadronic final states, J. Phys. G **42**, 103101 (2015).

[103] S. Marzani, G. Soyez, and M. Spannowsky, *Looking Inside Jets: An Introduction to Jet Substructure and Boosted-Object Phenomenology* (Springer, Berlin, 2019), Vol. 958.

[104] J. Collaboration, Jetscape/stat, https://github.com/JETSCAPE/STAT (2025).

[105] S. Cao *et al.* (JETSCAPE Collaboration), Determining the jet transport coefficient $\hat{q}$ from inclusive hadron suppression measurements using Bayesian parameter estimation, Phys. Rev. C **104**, 024905 (2021).

[106] R. Ehlers *et al.* (JETSCAPE Collaboration), Bayesian inference analysis of jet quenching using inclusive jet and hadron suppression measurements, Phys. Rev. C **111**, 054913 (2025).

[107] M. Aaboud, Jr. *et al.* (ATLAS Collaboration), Measurement of the nuclear modification factor for inclusive jets in Pb+Pb collisions at $\sqrt{s_{\rm NN}} = 5.02$ TeV with the ATLAS detector, Phys. Lett. B **790**, 108 (2019).

[108] S. Acharya *et al.* (ALICE Collaboration), Measurements of inclusive jet spectra in pp and central Pb-Pb collisions at $\sqrt{s_{\rm NN}} = 5.02$ TeV, Phys. Rev. C **101**, 034911 (2020).

[109] A. M. Sirunyan *et al.* (CMS Collaboration), First measurement of large area jet transverse momentum spectra in heavy-ion collisions, J. High Energy Phys. 05 (2021) 284.

[110] R. A. Soltz, D. A. Hangal, and A. Angerami, Simple model to investigate jet quenching and correlated errors for centrality-dependent nuclear modification factors in relativistic heavy-ion collisions, Phys. Rev. C **111**, 034911 (2025).

[111] J. Adam *et al.* (STAR Collaboration), Measurement of inclusive charged-particle jet production in Au + Au collisions at $\sqrt{s_{NN}} = 200$GeV, Phys. Rev. C **102**, 054913 (2020).

[112] V. Khachatryan *et al.* (CMS Collaboration), Charged-particle nuclear modification factors in PbPb and pPb collisions at $\sqrt{s_{\rm N\,N}} = 5.02$ TeV, J. High Energy Phys. 04 (2017) 039.

[113] S. Acharya *et al.* (ALICE Collaboration), Transverse momentum spectra and nuclear modification factors of charged particles in pp, p-Pb and Pb-Pb collisions at the LHC, J. High Energy Phys. 11 (2018) 013.

[114] G. Aad *et al.* (ATLAS Collaboration), Charged-hadron production in pp, $p+$Pb, Pb+Pb, and Xe+Xe collisions at $\sqrt{s_{\rm NN}} = 5$ TeV with the ATLAS detector at the LHC, J. High Energy Phys. 07 (2023) 074.

[115] J. Brewer, A. Huss, A. Mazeliauskas, and W. van der Schee, Ratios of jet and hadron spectra at LHC energies: Measuring high-p_T suppression without a pp reference, Phys. Rev. D **105**, 074040 (2022).

[116] P. Paakkinen, Light-nuclei gluons from dijet production in proton-oxygen collisions, Phys. Rev. D **105**, L031504 (2022).

[117] J. Gebhard, A. Mazeliauskas, and A. Takacs, No-quenching baseline for energy loss signals in oxygen-oxygen collisions, J. High Energy Phys. 04 (2025) 034.

[118] A. Mazeliauskas, Energy loss baseline for light hadrons in oxygen-oxygen collisions at $\sqrt{s_{\rm NN}} = 5.36$ TeV, arXiv:2509.07008.

[119] R. Katz, C. A. G. Prado, J. Noronha-Hostler, and A. A. P. Suaide, System-size scan of D meson R_{AA} and v_n using PbPb, XeXe, ArAr, and OO collisions at energies available at the CERN Large Hadron Collider, Phys. Rev. C **102**, 041901 (2020).

[120] A. Huss, A. Kurkela, A. Mazeliauskas, R. Paatelainen, W. van der Schee, and U. A. Wiedemann, Discovering partonic rescattering in light nucleus collisions, Phys. Rev. Lett. **126**, 192301 (2021).

[121] A. Huss, A. Kurkela, A. Mazeliauskas, R. Paatelainen, W. van der Schee, and U. A. Wiedemann, Predicting parton energy loss in small collision systems, Phys. Rev. C **103**, 054903 (2021).

[122] B. G. Zakharov, Jet quenching from heavy to light ion collisions, J. High Energy Phys. 09 (2021) 087.

[123] M. Xie, W. Ke, H. Zhang, and X.-N. Wang, Global constraint on the jet transport coefficient from single-hadron, dihadron, and γ-hadron spectra in high-energy heavy-ion collisions, Phys. Rev. C **109**, 064917 (2024).

[124] W. Ke and I. Vitev, Searching for QGP droplets with high-p_T hadrons and heavy flavor, Phys. Rev. C **107**, 064903 (2023).

[125] I. Vitev and W. Ke, Initial-state and final-state effects on hadron production in small collision systems, EPJ Web Conf. **296**, 15002 (2024).

[126] A. Ogrodnik, M. Rybář, and M. Spousta, Flavor and path-length dependence of jet quenching from inclusive jet and γ-jet suppression, Eur. Phys. J. C **85**, 899 (2025).

[127] W. van der Schee, I. Kolbé, G. Nijs, K. Ruhani, I. Ahmed, and S. Iqbal, Three models for charged hadron nuclear modification from light to heavy ions, arXiv:2509.04299.

[128] M. Rybczyński and W. Broniowski, Glauber Monte Carlo predictions for ultrarelativistic collisions with ^{16}O, Phys. Rev. C **100**, 064912 (2019).

[129] J. Casalderrey-Solana, Z. Hulcher, G. Milhano, D. Pablos, and K. Rajagopal, Simultaneous description of hadron and jet suppression in heavy-ion collisions, Phys. Rev. C **99**, 051901(R) (2019).

[130] A. Hayrapetyan *et al.* (CMS Collaboration), Discovery of suppressed charged-particle production in ultrarelativistic oxygen-oxygen collisions, arXiv:2510.09864.

[131] A. Takacs and D. Pablos, Bayesian constraints on pre-equilibrium jet quenching and predictions for oxygen collisions, https://github.com/adam-takacs/STAT (2026).

[132] A. V. Sadofyev, M. D. Sievert, and I. Vitev, *Ab initio* coupling of jets to collective flow in the opacity expansion approach, Phys. Rev. D **104**, 094044 (2021).

[133] Y. Fu, J. Casalderrey-Solana, and X.-N. Wang, Asymmetric transverse momentum broadening in an inhomogeneous medium, Phys. Rev. D **107**, 054038 (2023).

[134] J. a. Barata, A. V. Sadofyev, and C. A. Salgado, Jet broadening in dense inhomogeneous matter, Phys. Rev. D **105**, 114010 (2022).

[135] C. Andres, F. Dominguez, A. V. Sadofyev, and C. A. Salgado, Jet broadening in flowing matter: Resummation, Phys. Rev. D **106**, 074023 (2022).

[136] S. Hauksson and E. Iancu, Jet polarisation in an anisotropic medium, J. High Energy Phys. 08 (2023) 027.
[137] M. V. Kuzmin, X. Mayo López, J. Reiten, and A. V. Sadofyev, Jet quenching in anisotropic flowing matter, Phys. Rev. D **109**, 014036 (2024).
[138] S. P. Adhya and K. Tywoniuk, Sensitivity of jet quenching to the initial state in heavy-ion collisions, arXiv:2409.04295.
[139] J. Barata, S. Hauksson, X. Mayo López, and A. V. Sadofyev, Jet quenching in the glasma phase: Medium-induced radiation, Phys. Rev. D **110**, 094055 (2024).
[140] A. Altenburger, K. Boguslavski, and F. Lindenbauer, Jet broadening and radiation in the early anisotropic plasma in heavy-ion collisions, arXiv:2509.03868.
[141] F. Lindenbauer, Gluon splitting rates in an anisotropic plasma in the AMY formalism, arXiv:2509.09897.